Families of Granules, Flows, and Acoustic Events in the Solar Atmosphere from Hinode *Observations*

J.-M. Malherbe, T. Roudier, Z. Frank & M. Rieutord

Solar Physics
A Journal for Solar and Solar-Stellar Research and the Study of Solar Terrestrial Physics

ISSN 0038-0938

Sol Phys
DOI 10.1007/s11207-014-0630-7

ONLINE FIRST

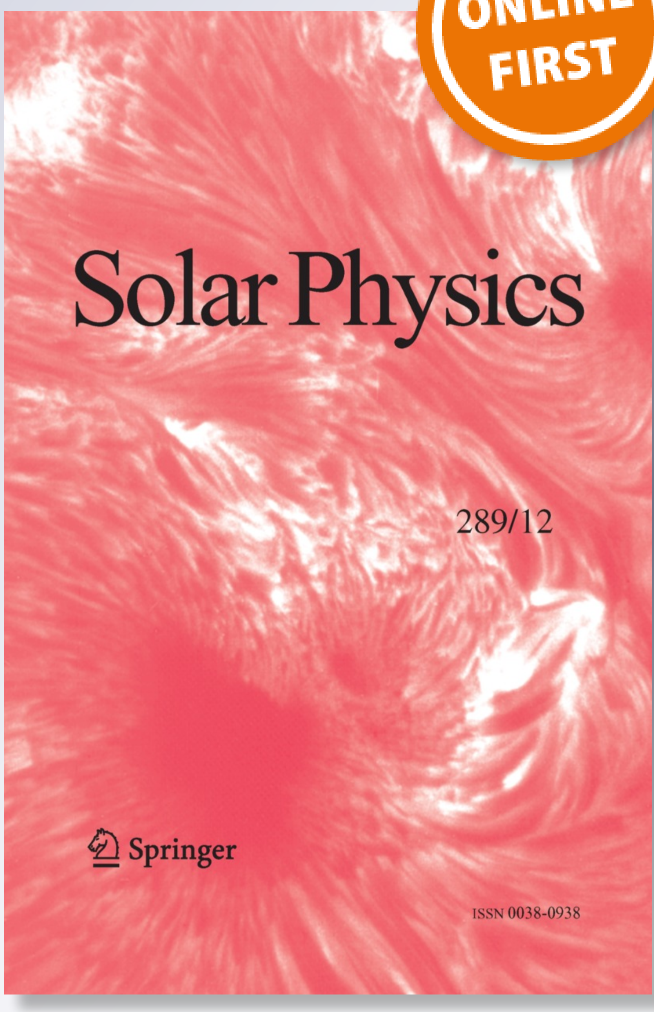

Springer

Solar Phys
DOI 10.1007/s11207-014-0630-7

Families of Granules, Flows, and Acoustic Events in the Solar Atmosphere from *Hinode* Observations

J.-M. Malherbe · T. Roudier · Z. Frank · M. Rieutord

Received: 19 June 2014 / Accepted: 12 November 2014

Abstract We investigate the relationship between trees of fragmenting granules (TFG), horizontal and vertical flows, and acoustic events (AE) in the photospheric network. AE are spatially concentrated and short-duration locations of acoustic energy flux. We performed observations at disk center of a 2D field of view (FOV) with high spatial and temporal resolutions provided by the *Solar Optical Telescope* onboard *Hinode*. Line profiles of Fe I 557.6 nm were recorded by the *Narrow-band Filter Imager* on an $80'' \times 36''$ FOV during five hours with a cadence of 22 seconds and $0.08''$ pixel size. Vertical velocities were derived at two atmospheric levels allowing the determination of the energy flux at the acoustic frequency of 3.3 mHz. Families of granules and horizontal velocities were obtained from local correlation tracking (LCT) after segmentation and labeling of either continuum intensities or granular Doppler shifts. AE exhibit durations in the range 0.25 to 1 hour compatible with the lifetime of families (80 % do not last more than two hours). High-energy AE have the shortest lifetimes. We found that most AE occur in intergranular lanes located in or close to the boundaries between different families (called inter families) in regions with predominantly downward vertical motions and horizontal converging flows. In contrast, diverging flows are observed inside families, with a few AE in the intergranules. At the beginning of the sequence, when families are not yet detected, the distribution of AE is not uniform and is

Electronic supplementary material The online version of this article (doi:10.1007/s11207-014-0630-7) contains supplementary material, which is available to authorized users.

J.-M. Malherbe (✉)
LESIA, Observatoire de Paris, 92195 Meudon, France
e-mail: Jean-Marie.Malherbe@obspm.fr

T. Roudier · M. Rieutord
IRAP, Université de Toulouse, CNRS, 14 Avenue Edouard Belin, 31400 Toulouse, France

T. Roudier
e-mail: Thierry.Roudier@ast.obs-mip.fr

Z. Frank
Lockheed Martin Solar and Astrophysics Laboratory, 3251 Hanover Street, Palo Alto, CA 94303, USA
e-mail: Zoe@lmsal.com

Published online: 29 November 2014

already organized at spatial lengths related to the mesogranular scale, with maximum contribution in the range 5″ to 10″, fully compatible with the scale of the maximum contribution of families in the TFG space. Although all sizes and durations seem to exist for families, their number decreases with increasing size and lifetime.

Keywords Granulation · Mesogranulation · Dynamics · Acoustic waves · Photosphere

1. Introduction

The contribution of the quiet Sun plays an important role in the general solar magnetism (Sheeley, 2005a, 2005b; Ossendrijver, 2003). One of the main goals in solar physics is to understand how magnetic flux is formed in the convective zone, then distributed, advected, and diffused over the surface. Addressing this question requires us to describe the physical nature of the flows, which may contribute to the transport of magnetic elements at various length scales. Many studies on the generation and evolution of magnetic-flux tubes have been performed during the last decade (Mackay and Yeates, 2012). From another point of view, several works have been devoted to the study of the dynamics of surface motions (horizontal flows) and their relationship to the magnetic field (Rieutord and Rincon, 2010). However, despite all of these efforts, the physical nature of the motions of the solar surface, magnetic transport, and diffusion processes is still poorly understood.

On one hand, an important step was the discovery of families of granules formed by successively exploding granules (lifetime around ten minutes) and originating from a single granule parent. Historically Kawaguchi (1980), studying the solar-granulation fragmentation with a temporal sequence obtained at the Pic du Midi Observatory in 1977, found evidence for the existence of families of granules produced from an initial fragmenting granule. Using the best available time sequence of the solar granulation, Roudier *et al.* (2003) demonstrated that a significant fraction of granules in the photosphere are organized in the form of trees of fragmenting granules (TFG), which can live several hours. The role played by TFG in the advection and diffusion of magnetic elements on the Sun surface was described by Roudier and Müller (2004). This result was confirmed by Roudier *et al.* (2009) with a long time sequence (48 hours) obtained with *Hinode* in the blue continuum. They showed the contribution of the TFG to the formation of the magnetic network. These results brought to light a strong relationship between the evolution of families and collective horizontal motions of magnetic elements in the quiet Sun. In particular, it was discovered that the magnetic flux was concentrated at the edge of families.

On the other hand, Doppler oscillations, which appear in vertical flows all over the Sun, are the second major component of the photospheric velocity field. Five-minute oscillations have been very closely studied, particularly to probe the physical properties of the solar interior. Recently, wave amplitude and phase diagnosis have been applied to detect acoustic events (AE) as sources of enhanced acoustic-wave generation at high spatial resolution (Brown, 1991). Acoustic-wave dissipation is assumed to be an important heating source for the lower atmosphere. AE appear as sub-arcsec space and time concentrated energy flux. They were first detected on high-resolution spectra from ground-based observations (Rimmele *et al.*, 1995; Strous, Goode, and Rimmele, 2000) and are now well studied by 2D spectrometers using line scans (Bello González *et al.*, 2010), now including *Hinode* (Malherbe *et al.*, 2012, hereafter Article I). However, previous works did not address the formation of AE with respect to TFG, because it is very difficult to obtain long and homogeneous observing sequences.

In this article we study the formation, distribution, and duration of AE (derived from Doppler measurements in Fe I 557.6 nm line at two altitudes) relative to granules, intergranules, and, for the first time, families of granules and interfamilies defined as the boundary lanes (also composed of intergranules) between different families. Relationships between horizontal flow patterns, AE and families are investigated.

2. Observations and Data Reduction

We used multi-wavelength data sets of the *Solar Optical Telescope* (SOT) onboard *Hinode* (*e.g.* Ichimoto *et al.*, 2005; Suematsu *et al.*, 2008). The SOT has a 0.50 m primary mirror aperture with a spatial resolution of about 0.3″ at 550 nm. Observations were performed at disk center, so that vertical velocities produce Doppler shifts, whereas horizontal velocities can be derived from the proper motions of granules.

We used the *Narrow-band Filter Imager* (NFI) to scan profiles of the magnetically insensitive 557.6 nm Fe I line with a spatial resolution of 0.3″. The full width at half maximum of the filter is 6 pm. The spectral line was scanned using seven wavelengths along the line profile in the following order, with respect to the line center: −12, −8, −4, 0, +4, +8, +12 pm. The observations were recorded continuously on 14 April 2010, from 06:40 to 11:50 UT. Each line scan took 22 seconds for a total observing time of more than five hours, so that we have 846 consecutive times of observations. The field of view (FOV) was 82″ × 41″ (1024 × 512 pixels) with a pixel sampling of 0.08″.

We first aligned images corresponding to the blue wing of the line at −12 pm away from line center using cross correlation. Then we co-aligned the seven consecutive spectral images (−12 to +12 pm by 4 pm step) covering the line and belonging to the same scan by correlating two successive images spectrally separated by 4 pm. The procedure reduced the FOV to 80″ × 36″ and is detailed in Article I. Let us summarize the main steps:

i) A phase correction was applied to the temporal Fourier transform of the data set for each wavelength of the line scan, with respect to the first wavelength (−12 pm), in order to correct the time shift (2.4 seconds) between them.
ii) Each intensity image of the series was deconvolved with the modulation transfer function (MTF) of the telescope and the CCD array.
iii) Radial velocities and intensities at different depths in the line profile were obtained using the bisector technique. We defined two bisectors (chords) of 8 pm (line core) and 12 pm (inflection points) corresponding, respectively, to atmospheric levels at about 130 km and 180 km (see Article I). Doppler shifts and intensity fluctuations were obtained by reference to the mean profile. The Doppler shifts provided the vertical component [v_z] of the velocity; from [v_z] at both altitudes, we obtained an approximate value of the vertical gradient [$\partial v_z/\partial z$].
iv) From radial velocities at two heights, we derived phases and amplitudes of vertically traveling waves and the acoustic flux as a function of time and space. The acoustic flux [e] per unit surface is defined by the product of an energy density and the group velocity, assuming that the density [ρ] is constant: $e \propto \rho v_z^2 v_{\mathrm{g}}$ where $|v_z|$ is the amplitude and v_{g} is the group velocity of the wave. The value of v_{g} cannot be deduced directly from observations. We used instead the relation $v_{\mathrm{g}} v_{\varphi} = C_{\mathrm{s}}^2$, where v_{φ} is the phase velocity and $C_{\mathrm{s}} = \sqrt{\gamma P/\rho}$ is the adiabatic sound speed [P is the pressure and $\gamma = 5/3$]. $v_{\varphi} = \omega/k_z$ was derived from observations using $k_z = \Delta\varphi/\Delta z$ where ω is the frequency of the wave and $\Delta\varphi$ the phase lag inside the layer of thickness Δz. The energy flux given

by $e \propto v_z^2(\gamma P/\omega)(\Delta\varphi/\Delta z)$ was computed at 3.3 mHz (bandwidth 1.8 mHz). For that purpose $|v_z|$ and $\Delta\varphi$ were derived from Doppler shifts using the Hilbert transform at two altitudes.

Granules were identified in intensity after oscillation filtering of the far wings of Fe I 557.6 nm in the k–ω space (frequencies corresponding to $\omega \geq C_s k$, where $C_s = 6\ \mathrm{km\,s^{-1}}$ is the sound speed and $k = \sqrt{k_x^2 + k_y^2}$ is the horizontal wave number, were suppressed). The same procedure (except for AE) was applied to Doppler shifts to get permanent vertical flows at two altitudes. Then a segmentation was applied to the 846 intensity images. In order to detect the formation of TFG or families, granules were labeled in time as described by Roudier *et al.* (2003). TFG (repeatedly splitting granules originating from a single parent) are an appropriate tool to quantify the temporal and spatial organization of the solar granulation at larger scales (a few arcsec). It was suggested by Roudier *et al.* (2003) that families correspond to mesogranules (although the existence of mesogranules remains controversial). Granules belonging to a given TFG were labeled with the same number. Families need several hours to be tracked by that method (which requires a long observing sequence), but we will see that the spatial distribution of AE reveals their existence before their detection.

Horizontal velocities were computed from proper motions of granules observed in the far wings (average between positions at −12 pm and +12 pm apart from line center) after removal of intensity oscillations filtered in the k–ω space. We used local correlation tracking (LCT) as described by November and Simon (1988) in order to measure horizontal velocities v_x and v_y as a function of space and time. From v_x and v_y, we derived $v^2 = v_x^2 + v_y^2$ and the horizontal divergence $[\partial v_x/\partial x + \partial v_y/\partial y]$ of the flow.

Doppler shifts have the spatial (0.3″) and temporal (22 seconds) resolution of the original data; but, this is not the case for horizontal velocities. The tracking method requires us to average granular motions over a minimum spatial [3″] and temporal [30 minutes] window such that the length scale and time scale are much greater. Only overall flows are detected, implying that Doppler shifts and horizontal motions cannot be combined together to get the instantaneous velocity vector.

We built several movies, provided as Electronic Supplemental Material (ESM), using the 846 time steps that show the evolution of families, velocities, AE and other related quantities (see the Appendix for more details).

3. Families and Vertical and Horizontal Flows

Figure 1 (and ESM movie 1) shows families together with vertical velocities (Doppler shifts) at the end of the sequence when families are well developed. In the k–ω space, we filtered all frequencies (oscillations) in order to keep only permanent convective flows. Downward velocities are observed in intergranular (−0.45 $\mathrm{km\,s^{-1}}$ median value) and interfamily lanes (−0.35 $\mathrm{km\,s^{-1}}$ median), while upward motions (+0.4 $\mathrm{km\,s^{-1}}$ median) are present in granules.

Figure 2 (and ESM movie 2) shows families together with vertical gradients of Doppler shifts. We defined the gradient as the velocity difference between two altitudes (so that it is measured in $\mathrm{km\,s^{-1}}$) corresponding to the formation height of line core and inflection points. As found in Article I, intergranular regions exhibit mostly positive (upward) gradients of about +0.05 $\mathrm{km\,s^{-1}}$ (median value) while granules and their interior have rather negative gradients of about −0.05 $\mathrm{km\,s^{-1}}$ (median) through a layer of thickness 50 km.

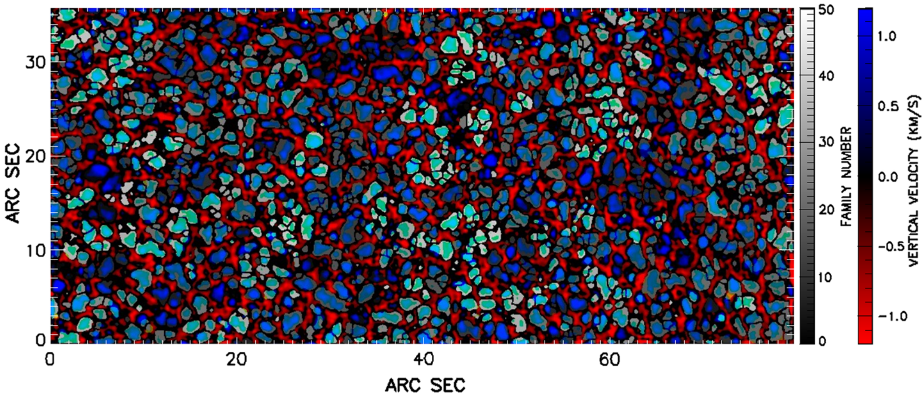

Figure 1 Families of granules at the end of the sequence. Granules belonging to the same family are displayed with uniform gray level (identifying the family number, and not intensity, while intergranules are black). In addition, the gray levels are modulated by Doppler shifts (blue/red for upward/downward velocities). FOV $= 80'' \times 36''$. Pixel size $0.08''$.

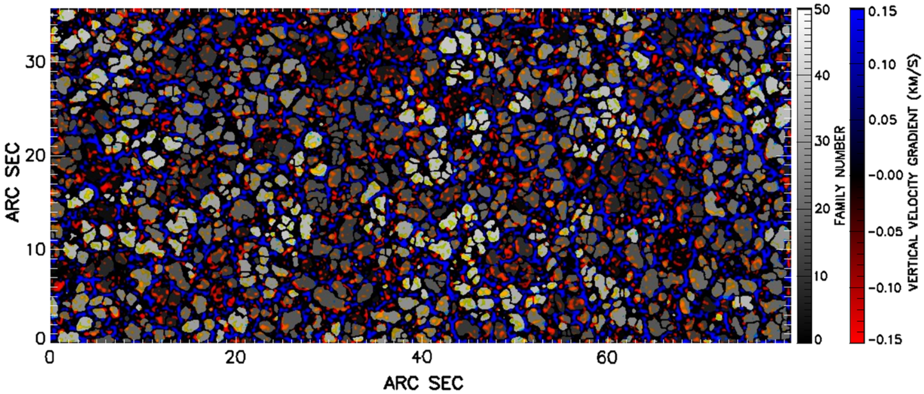

Figure 2 Families of granules at the end of the sequence. Granules belonging to the same family are displayed with uniform gray level (identifying the family number, not intensity, while intergranules are black) modulated by the vertical gradient of Doppler shifts (blue/red for positive/negative, the gradient is defined as the velocity difference between the upper and lower level of observations). FOV $= 80'' \times 36''$. Pixel size $0.08''$.

Figure 3 (and ESM movie 3) shows interfamilies (intergranules separating granules belonging to distinct families) together with the horizontal velocity and AE. Families match most cells of horizontal flows while interfamilies are rather near the border of velocity cells (see for instance families at coordinates x, y: 10, 20; 20, 22; 30, 15). The median speed of the cells is about 0.4 $\mathrm{km\,s^{-1}}$. Most AE take place in inter family lanes or very close in the form of spatially concentrated structures (a few pixels of $0.08''$).

Figure 4 (and ESM movie 4) shows interfamily boundaries at the end of the sequence together with the divergence of horizontal velocities and AE. Families include most cells of diverging flows and some converging flows (see for instance families at coordinates x, y: 10, 22; 32, 21; 72, 23), while interfamily boundaries are generally above or close to converging regions, so that AE, mostly associated with interfamilies, are also correlated with converging flows.

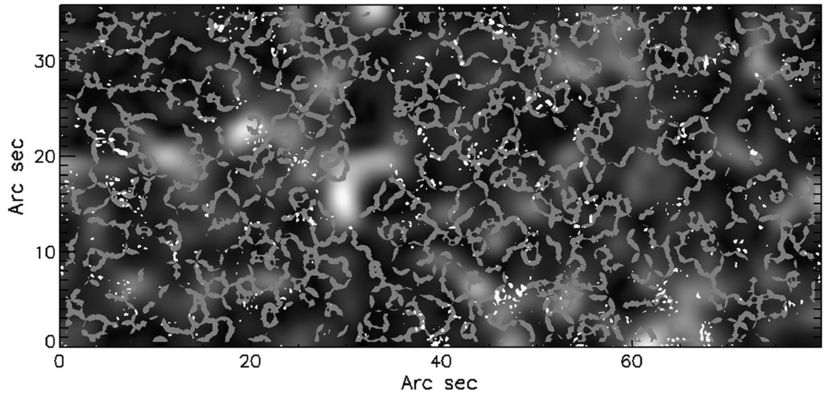

Figure 3 Interfamily boundaries of granules at the end of the sequence (uniform gray lanes) and AE (white points corresponding to the absolute value of the acoustic flux). The background (gray levels) represents the square of the horizontal velocity vector $v^2 = v_x^2 + v_y^2$. FOV $= 80'' \times 36''$. Pixel size $0.08''$.

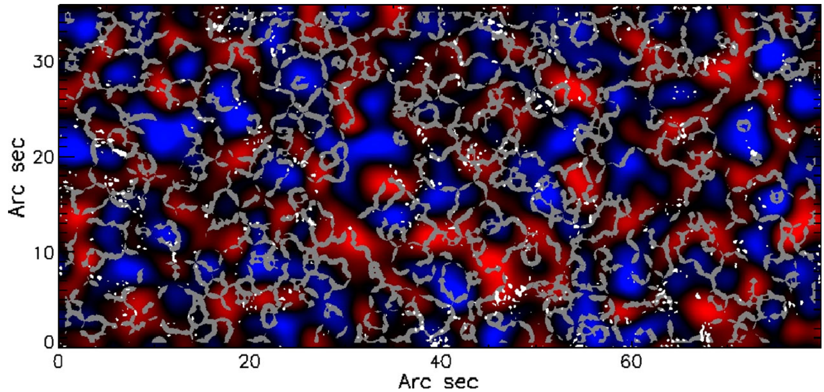

Figure 4 Interfamily boundaries of granules at the end of the sequence (uniform gray lanes) and AE (white points). The background displays the divergence $[\partial v_x/\partial x + \partial v_y/\partial y]$ of the horizontal velocity vector (blue/red for diverging/converging areas). FOV $= 80'' \times 36''$. Pixel size $0.08''$.

4. Characteristics of Families

We studied the lifetime of families of the FOV (Figure 5) for comparison with AE (next section) and found that there is no characteristic lifetime (as the distribution function can be fitted by an exponential law) but there is a relationship between the lifetime and the average size of the families. Long-duration families are clearly the most extended, while small families are ephemeral. Our analysis shows that 50 % of families have lifetimes shorter than one hour, and 80 % shorter than two hours, so that the order of magnitude is the hour, intermediate between the well known granulation lifetime (ten minutes) and the supergranulation (about 24 hours). Although our sequence is not long enough to see the full development of families, our results corroborate those obtained by Roudier *et al.* (2003) using an 11-hour sequence (in the broad band and blue continuum) from the *Swedish Vacuum Solar Telescope* (SVST/La Palma).

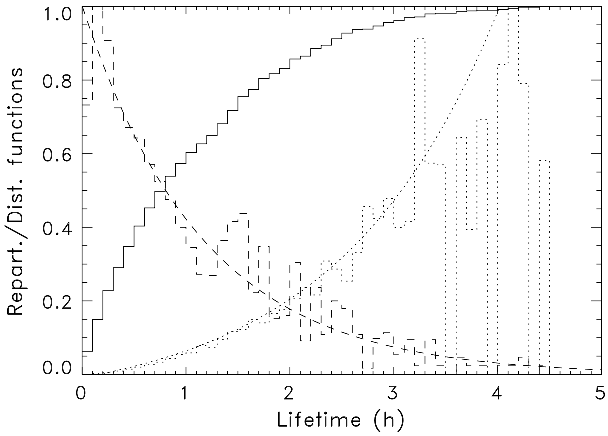

Figure 5 Distribution functions of the lifetime [hours] of families (dashed line) and of the volume of families in the TFG space (x, y, t, dotted line) with the respective exponential fits (arbitrary units); distribution function of lifetimes (solid line).

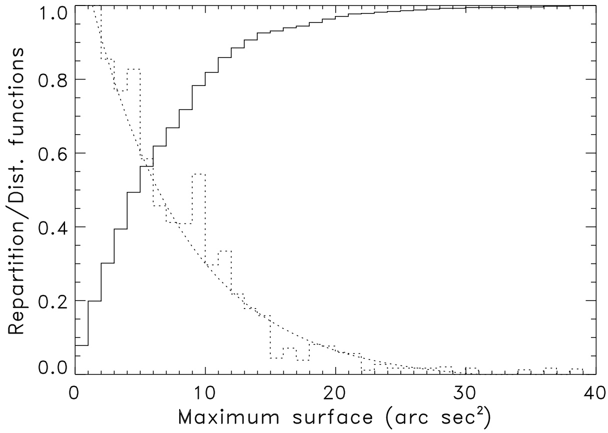

Figure 6 Distribution function of the size of families in arcsec^2 (dotted line, with exponential fit, arbitrary unit) and distribution function (solid line).

Figure 6 provides the statistics of family sizes: as for lifetime, there is no characteristic size. In the FOV, all sizes between 1 arcsec^2 to 40 arcsec^2 are observed (approximately 1 to 40 granules), but the number of families decreases continuously with size (exponential distribution). 95 % of families have an area smaller than 20 arcsec^2 (and 50 % are smaller than 7 arcsec^2).

The size of families varies in time and there is often a short growth and longer decay phase (except for very small and ephemeral families): for example, Figure 7 shows the evolution of the area of some typical families as a function of time for lifetimes of 0.5, 1, 2, 4 hours or more (the shortest-lived families are the most numerous).

We have investigated the contribution of families quantified by their pseudo volume (integral of family area over time in arcsec^2 hour) in the TFG 3D space (x, y, t) as a function of their mean or maximum size. Figure 8 indicates that families with mean areas in the range 3 arcsec^2 to 10 arcsec^2 (maximum areas in the range 5 arcsec^2 to 25 arcsec^2) have the most significant contribution in the TFG space. It must be noticed that these values are lower limits, as the sequence duration is not long enough to display the full development of families.

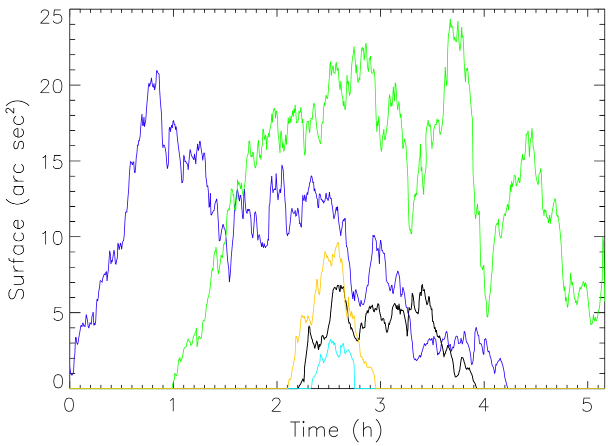

Figure 7 Surface in arcsec^2 of five typical families with various durations as a function of time [hours].

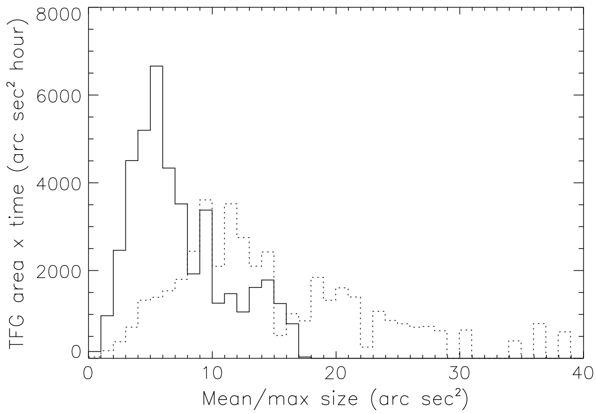

Figure 8 Volume of families in the TFG space as a function of mean (solid line) or maximum (dotted line) area.

5. Acoustic Events and Families

AE together with families of granules are shown in Figures 9 and 10 (and ESM movies 5, 6, and 7). The net acoustic flux is directed upwards even if some downward flux does exist. Most AE occur in intergranular regions and more specifically at the boundaries or close to the frontiers between two different families (called inter families). In Figure 9 (and ESM movie 5), where only AE are represented, one clearly sees that the distribution of AE is not uniform but corresponds to the characteristic length scale of mesogranules (5″ to 10″). Even if families are not formed at the starting point of the sequence (ESM movies 6 and 7), because the algorithm needs a few hours to detect successively fragmenting granules and the birth of TFG, they are well established at the beginning of the sequence through the spatial organization of AE. Hence, AE allow us to delineate families before they are revealed in intensity by the segmentation and labeling process.

We tried to quantify the spatial distribution of AE using a segmentation process to measure the distance between them. As for families, Figure 11 shows that there is no characteristic size, but the distribution of the product (distance × number of corresponding AE) reveals the existence of the two contributions visible in Figure 9: a 5″ to 10″ distance corresponding to the typical mesogranular scale and a secondary peak around 1″ corresponding to the size of granules.

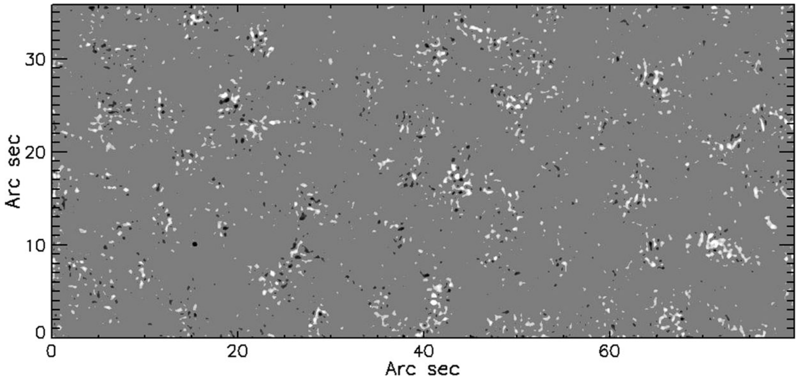

Figure 9 Distribution of AE at the beginning of the sequence (white/black for upward/downward flux). FOV = 80″ × 36″. Pixel size 0.08″.

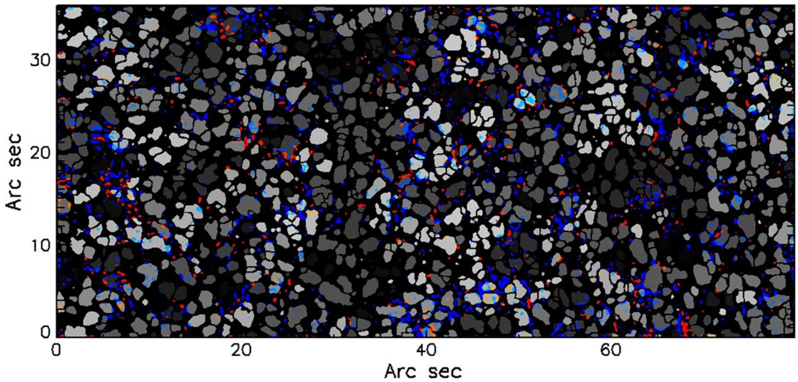

Figure 10 Families of granules at the end of the sequence (granules belonging to the same family have uniform gray level corresponding to the family number) and AE (blue/red for upward/downward flux). FOV = 80″ × 36″. Pixel size 0.08″.

A statistical analysis was also performed to determine the location of AE *versus* intergranules and interfamilies and the results are displayed in Figure 12. It shows that 70 % of AE are located exactly inside intergranular lanes and 90 % of AE are within 0.2″, so there is a clear association between intergranular lanes and AE. However, the figure also reveals that, although only 25 % of AE are located exactly in interfamily lanes, 90 % are within 0.8″ of these structures (a distance comparable to typical granule sizes). We conclude that AE form 90 % of the time in the vicinity of interfamilies, at the boundary between families or within a very short distance. The spatial distribution of AE appears strongly related to the spatial organization of families, giving a new role to the mesogranular scale in the propagation of energy flux towards the chromosphere.

We investigated (Figure 13) the lifetime of AE present in the FOV. We took for that purpose the duration of AE above three thresholds corresponding to 40 %, 50 %, and 60 % of their maximum energy. The median lifetime was found to be, respectively, 2100, 1600, and 1200 seconds. Durations extend typically from a quarter to one hour; AE lifetimes are shorter than, but of the same order of magnitude as, those of families. We also examined

Figure 11 Distribution of the distance between AE (solid line) and of the product of distance × number of corresponding AE (dashed line).

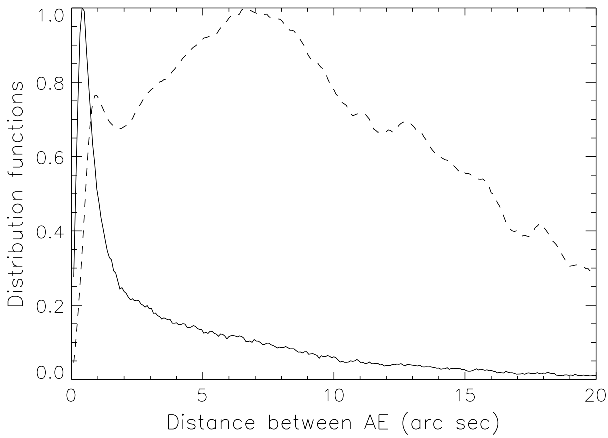

Figure 12 Distribution functions of acoustic events as a function of distance to intergranules (top curves) and interfamilies (bottom curves). For each set of curves, different thresholds were applied to the energy flux of AE, showing that this parameter does not play a significant role.

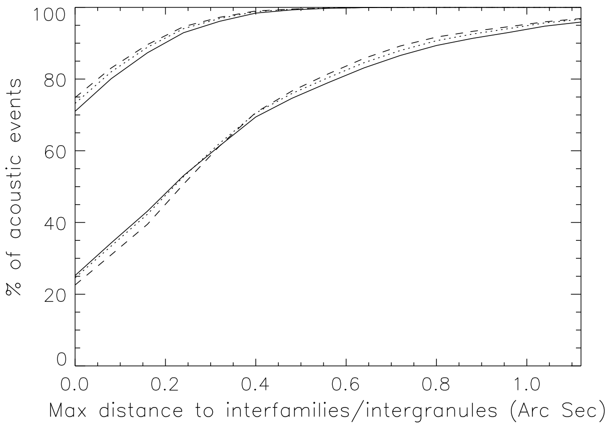

lifetimes *versus* maxima of energy flux reached during each event. We found that the most energetic events are also the shortest.

Figure 14 presents the typical evolution of energy flux in AE as a function of time. Several peaks with lifetimes of half an hour may occur. In most cases, AE appear in converging regions (negative divergence). Divergences were derived from horizontal motions of intensity structures (granulation in line wing) as well as motions of Doppler structures (upward velocity pattern of granules), providing similar results.

The distribution of AE was finally studied in relation to vertical, and horizontal motions and divergences. For that purpose, we filtered oscillations in the k–ω space in order to keep only permanent flows. We found that most AE are associated with downward motions in intergranules as well as in interfamilies ($-0.3\ \mathrm{km\,s^{-1}}$ average, $0.4\ \mathrm{km\,s^{-1}}$ standard deviation). About 75 % of the flux is concentrated in these regions where the vertical gradient of velocities is also positive (velocity difference of $0.03\ \mathrm{km\,s^{-1}}$ along 50 km variation) and where horizontal velocities have a mean value of $0.4\ \mathrm{km\,s^{-1}}$ ($0.2\ \mathrm{km\,s^{-1}}$ standard deviation). We found also that about 60 % of the flux is concentrated in converging regions ($-10^{-4}\ \mathrm{s^{-1}}$ average).

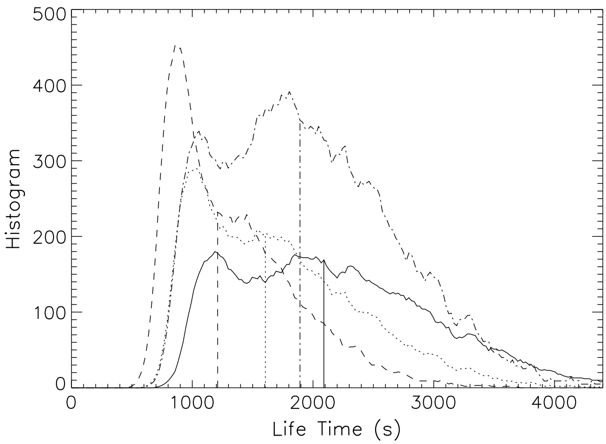

Figure 13 Distribution function of AE lifetime [seconds] for three thresholds (duration above 40 %, 50 %, 60 % of maximum energy for, respectively, solid, dotted, and dashed lines).

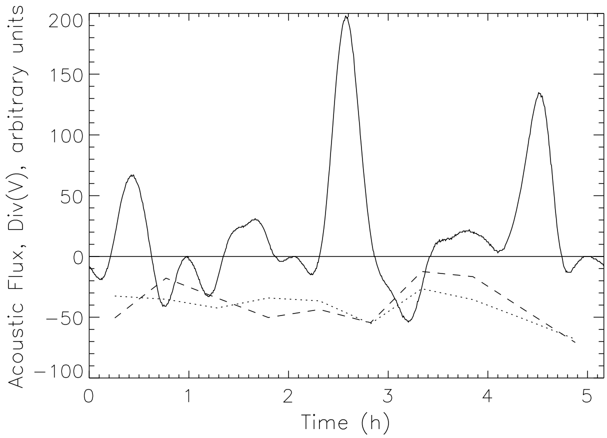

Figure 14 Energy flux of a typical AE (solid line, arbitrary unit) as a function of time [hours]; velocity divergence (dotted/dashed lines for divergences derived from, respectively, intensity/Doppler structures, arbitrary units).

6. Conclusion

Acoustic events are evident from images taken by the SOT/NFI onboard *Hinode* with outstanding spatial resolution and FOV ($80'' \times 36''$) using a non-magnetic five-hour sequence of the Fe I 557.6 nm line scans with 22-second temporal resolution. Vertical velocities were computed at two altitudes corresponding to different chords in the line profiles, using the bisector technique. The group velocity is proportional to the phase lag and was used to compute the signed energy flux. Families (or TFG) were obtained after segmentation and time labeling. Horizontal velocities were detected from granular motions through the LCT method (either from their intensity shape or Doppler shift structure) and divergences were derived.

AE are ephemeral and small-scale objects with typical size of $0.3''$ (or less). Their median duration is about 1600 seconds (range 0.25 to 1 hour). The spatial distribution of AE matches families (TFG) of granules. Most occur in intergranular and more precisely in interfamily lanes (boundaries between different families), downward velocity regions (redshifts), and areas of converging flows, while diverging areas are located more often inside family cells. The family lifetime was studied and we found values of the same order of magnitude as the duration of AE. 80 % of families exhibit lifetimes shorter than two hours. There is no characteristic area for families: all areas exist in the range 1 arcsec^2 to 40 arcsec^2 but the number of families decreases with size and lifetime (exponential distributions). Nevertheless, we found that the most significant contribution in the TFG space is the mesogranular scale, in agreement with the most significant distance between AE in interfamilies [5″ to 10″].

The MHD numerical simulation of these phenomena is a difficult challenge. Nevertheless, interactions between magnetic fields on the one hand, and families, velocity fields and AE on the other hand, still need to be studied. In particular, it would be of great interest to correlate AE with the evolution of families and magnetic elements, in relation with larger scales such as supergranulation which is likely structured by magnetic fields in the quiet Sun (Roudier and Müller, 2004; Rincon and Rieutord, 2003). This aim requires new observations, which will be carried out soon by *Hinode* with NFI scans of the Na D_1 589.6 nm line (using analysis of the circular polarization, providing Doppler velocities and magnetic fields) and BFI blue continuum images (allowing the determination of horizontal photospheric velocities).

Acknowledgments We are indebted to the *Hinode* team for the possibility to use their data. *Hinode* is a Japanese mission developed and launched by ISAS/JAXA, collaborating with NAOJ as a domestic partner, NASA and STFC (UK) as international partners. Scientific operation of the *Hinode* mission is conducted by the *Hinode* science team organized at ISAS/JAXA. This team mainly consists of scientists from institutes in the partner countries. Support for the post-launch operation is provided by JAXA and NAOJ (Japan), STFC (UK), NASA, ESA, and NSC (Norway). The authors thank the anonymous referee for helpful comments and suggestions. This work was supported by the Centre National de la Recherche Scientifique (C.N.R.S.), France.

Appendix

The Electronic Supplemental Material movies consist of 846 images of 998 × 448 pixels and are available either in MPEG1 or MPEG4 format (better quality). The acceleration factor is about 660 for MPEG1 and 275 for MPEG4. The pixel size is 0.08″ and the time step is 22 seconds. For horizontal velocities and divergences, the spatial and temporal resolutions are reduced, respectively, to 3″ and 30 minutes; interpolations were used.

- Movie 1: Families of granules and Doppler shifts in Fe I 557.6 nm. Granules belonging to the same family have a uniform gray level corresponding to the family number. Families can be identified as mesogranules. Doppler velocities appear in blue/red for, respectively, upward/downward motions and affect both granules (mainly upward) and intergranules (mostly downward). Families detected by the LCT need several hours to appear.
- Movie 2: Families of granules and Doppler gradient in Fe I 557.6 nm. Vertical gradients (through a 50 km layer) of velocities (core/inflection point difference) appear in blue/red, respectively, for positive/negative values. Positive gradients are dominant in intergranules.
- Movie 3: Interfamilies, horizontal motions and AE. The boundaries between families of granules (interfamilies) are shown in gray. AE (white) form close to interfamilies. Quadratic horizontal velocities appear in gray levels with maxima mostly located inside families.
- Movie 4: Interfamilies, divergence of horizontal velocities, and AE. Diverging/converging areas are, respectively, blue/red. Most diverging regions are located inside families, while boundaries (interfamilies) together with AE are more often associated to converging patterns.
- Movie 5: AE are flux concentrations in space and time with lifetime in the range 0.25 to 1 hour. Upward/downward flux is shown, respectively, in white/black. The spatial distribution is not uniform: most of the flux is located near the boundaries between TFG (interfamilies at mesogranular scale).

- Movie 6: Families of granules (gray levels) and AE. The major part of the flux (upward/downward, respectively, in blue/red) occur in intergranular lanes close to the boundaries between families (interfamilies). AE and families have lifetimes of the same order of magnitude.
- Movie 7: Families of granules and AE. Granules belonging to the same family have uniform color. Most AE (white) appear in dark intergranular regions close to the boundaries between families.

References

Bello González, N., Franz, N., Martinez Pillet, V., Bonet, J.A., Solanki, S.K., del Toro Iniesta, J.C., Schmidt, W., Gandorfer, A., Domingo, V., Barthol, P., *et al.*: 2010, *Astrophys. J. Lett.* **723**, L134. DOI.

Brown, T.M.: 1991, *Astrophys. J.* **371**, 396. DOI.

Ichimoto, K., Tsuneta, S., Suematsu, Y., Shimizu, T., Otsubo, M., Kato, Y., *et al.*: 2005, In: Mather, J.C. (ed.) *Optical, Infrared, and Millimeter Space Telescopes*, *Proc. SPIE* **5487**, 1142.

Kawaguchi, I.: 1980, *Solar Phys.* **65**, 207. DOI.

Mackay, D., Yeates, A.: 2012, *Living Rev. Solar Phys.* **9**, 6. DOI.

Malherbe, J.M., Roudier, T., Rieutord, M., Berger, T., Frank, Z.: 2012, *Solar Phys.* **278**, 241. DOI.

November, L.J., Simon, G.W.: 1988, *Astrophys. J.* **333**, 427. DOI.

Ossendrijver, M.: 2003, *Astron. Astrophys. Rev.* **11**, 287. DOI.

Rieutord, M., Rincon, F.: 2010, *Living Rev. Solar Phys.* **7**, 2. DOI.

Rimmele, T.R., Goode, P.R., Harold, E., Stebbins, R.T.: 1995, *Astrophys. J. Lett.* **444**, L119. DOI.

Rincon, F., Rieutord, M.: 2003, In: Combes, F., Barret, D., Contini, T., Pagani, L. (eds.) *SF2A*, EdP-Sciences, Les Ulis, 103.

Roudier, T., Müller, R.: 2004, *Astron. Astrophys.* **419**, 757. DOI.

Roudier, T., Lignières, F., Rieutord, M., Brandt, P.N., Malherbe, J.M.: 2003, *Astron. Astrophys.* **409**, 299. DOI.

Roudier, T., Rieutord, M., Brito, D., Rincon, F., Malherbe, J.M., Meunier, N., Berger, T., Frank, Z.: 2009, *Astron. Astrophys.* **495**, 945. DOI.

Sheeley, N.R.: 2005a, In: Fleck, B., Zurbuchen, T.H., Lacoste, H. (eds.) *Solar Wind 11/SOHO 16, Connecting Sun and Heliosphere*, *ESA* **SP-592**, 233. ISBN 92-9092-903-0.

Sheeley, N.R.: 2005b, *Living Rev. Solar Phys.* **2**, 5. DOI.

Strous, L.H., Goode, P.R., Rimmele, T.R.: 2000, *Astrophys. J.* **535**, 1000. DOI.

Suematsu, Y., Tsuneta, S., Ichimoto, K., Shimizu, T., Otsubo, M., Katsukawa, Y., *et al.*: 2008, *Solar Phys.* **249**, 197. DOI.